A synthetic optically pumped gradiometer for magnetocardiography measurements*

Shu-Lin Zhang(张树林)[1,2,3,†] and Ning Cao(曹宁)[1,4]

[1] *Joint Laboratory of Bioimaging Technology and Applications, CAS–SIMIT & MEDI, Shanghai* 201899, *China*
[2] *State Key Laboratory of Functional Materials for Informatics, Institute of Microsystem and Information Technology (SIMIT), Chinese Academy of Sciences (CAS), Shanghai* 200050, *China*
[3] *Centre for Excellence in Superconducting Electronics, Chinese Academy of Sciences, Shanghai* 200050, *China*
[4] *Shanghai Medi Instruments Ltd., Shanghai* 201899, *China*

(Received 13 December 2019; revised manuscript received 8 February 2020; accepted manuscript online 20 February 2020)

Magnetocardiography (MCG) measurement is important for investigating the cardiac biological activities. Traditionally, the extremely weak MCG signal was detected by using superconducting quantum interference devices (SQUIDs). As a room-temperature magnetic-field sensor, optically pumped magnetometer (OPM) has shown to have comparable sensitivity to that of SQUIDs, which is very suitable for biomagnetic measurements. In this paper, a synthetic gradiometer was constructed by using two OPMs under spin-exchange relaxation-free (SERF) conditions within a moderate magnetically shielded room (MSR). The magnetic noise of the OPM was measured to less than 70 fT/Hz$^{1/2}$. Under a baseline of 100 mm, noise cancellation of about 30 dB was achieved. MCG was successfully measured with a signal to noise ratio (SNR) of about 37 dB. The synthetic gradiometer technique was very effective to suppress the residual environmental fields, demonstrating the OPM gradiometer technique for highly cost-effective biomagnetic measurements.

Keywords: optically pumped magnetometer (OPM), magnetocardiography (MCG), gradiometer

PACS: 07.07.Df, 87.85.Ox, 07.55.Ge **DOI:** 10.1088/1674-1056/ab7801

1. Introduction

Magnetocardiography (MCG) is a contactless, non-invasive imaging technique to record the magnetic fields generated by the human heart.[1] It can visualize the myocardium activities by mapping the magnetic fields over the thorax area. The clinical trials have reported that MCG can provide a high diagnostic accuracy for many heart diseases, such as coronary artery disease (CAD), ischemic heart disease (IHD), arrhythmia, *etc*.[2–4] Especially, it was proved to be very valuable for the rapid screening of IHD.[5,6]

The MCG signal is extremely weak. As a highly sensitive magnetic sensor, superconducting quantum interference devices (SQUIDs) are commonly used.[7] Currently, several SQUID-based MCG systems have been commercialized and put into clinics worldwide. Despite the high sensitivity of SQUID sensors, they require liquid helium to maintain the working temperature of 4.2 K. This expensive running cost makes SQUID-based MCG systems less attractive for clinical applications. During the past few years, the optically pumped magnetometers (OPMs) have emerged to be the most attractive room-temperature magnetic sensors.[8,9] Under spin-exchange relaxation-free (SERF) conditions, OPMs can achieve a high sensitivity comparable to that of SQUIDs.[10,11]

In order to preserve a higher sensitivity, OPMs under SERF conditions must be operated under a well shielded environment. Within a magnetically shielded room (MSR) or tube, biomagnetic measurements were successfully conducted by using OPMs, such as MCG, magnetoencephyalography (MEG), *etc*.[12–15] However, there is still environmental disturbance although using a moderate MSR. Considering the expensive shielding costs, the popular used gradiometer techniques like SQUID systems will be a compromise method. Therefore, it will be very valuable to evaluate the gradient optically pumped measurements for the residual noise cancellation.

In this paper, a synthetic gradiometer method was conducted for MCG measurements. It was performed by using two individual OPMs under the SERF conditions, which were regarded as signal sensor and reference respectively. The OPM output was synthesized by using a least square algorithm with a constant subtraction coefficient. Within a moderate MSR, the gradiometer method is shown to be very effective for noise cancellation and MCG measurements, which will be applicable for developing low-cost OPM-based MCG systems.

2. Experimental setup

The schematic diagram of the experimental setup is shown in Fig. 1. The experiments are performed within a mod-

*Project supported by the National Natural Science Foundation of China (Grant No. 61701486).
†Corresponding author. E-mail: zhangsl@mail.sim.ac.cn

erate MSR with two-layer permalloy. Two OPMs were used to synthesize a gradiometer. The lower one was configured as a sensor to detect MCG signal, and the upper one was the reference. The baseline was set to be 100 mm, which was longer enough for MCG measurements.

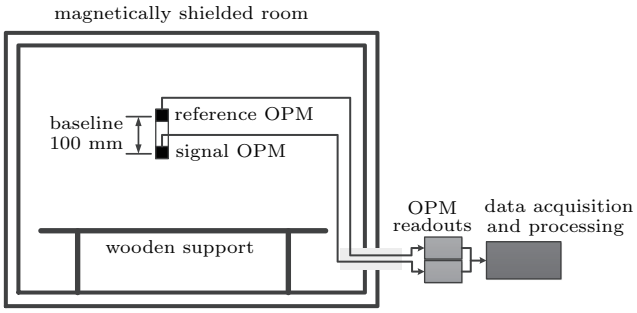

Fig. 1. Schematic diagram of the experimental setup.

We employed commercial OPMs under SERF conditions (QuSpin Inc., Louisville, CO, USA) to make the measurements. It has a configuration of a typical noise level of 10 fT/Hz$^{1/2}$, a bandwidth larger than 100 Hz, a dynamic range of about 50 nT, and a size of 12.4 mm×16.6 mm× 24.4 mm. The basic configuration of the OPM is shown in Fig. 2. The OPM head contains all the necessary optical components, including a semiconductor laser for optical pumping, optics for laser beam conditioning, a vapour cell, and a silicon photodiode. The sensor head connects to the electronic readouts via a 5-m cable, which is placed outside the MSR to minimize magnetic interferences. The scaling of output voltage to magnetic field is set to 0.89 V/nT.

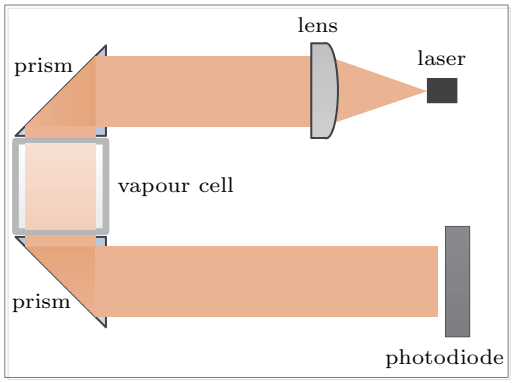

Fig. 2. The basic configuration of the OPM.

The analog outputs of OPMs along the vertical direction were digitized by a 24-bit 4-channel data acquisition (DAQ) system at a sample rate of 2 kHz. The raw data were preprocessed by using a 45-Hz low-pass filter to eliminate the powerline interference, which was sufficient to observe the main components of the cardiac activities. Afterwards, a synthetic gradiometer was constructed by

$$G_{\mathrm{syn}} = B_{\mathrm{s}} - k \cdot B_{\mathrm{r}}, \tag{1}$$

where G_{syn}, B_{s}, and B_{r} are the outputs of the synthetic gradiometer, signal OPM, and reference OPM respectively. k is the subtraction coefficient. It was obtained by using a least square algorithm and given by

$$k = \frac{\sum_{i=1}^{N} B_{\mathrm{si}} \cdot B_{\mathrm{ri}}}{\sum_{i=1}^{N} B_{\mathrm{ri}} \cdot B_{\mathrm{ri}}}, \tag{2}$$

where B_{si} and B_{ri} are the digital data with a total length of N. Based on the above process, the gradient MCG signal can be obtained.

3. Results and discussion

Before the MCG experiments, the power spectral density noise of the OPMs was measured firstly by using a dynamic signal analyzer, as shown in Fig. 3. The magnetic field noise was measured to be 65 fT/Hz$^{1/2}$ and 54 fT/Hz$^{1/2}$ for the signal and reference OPMs respectively. It was 5 times larger than the given noise level by QuSpin. The reason may be attribute to the non-ideal working environments, such as magnetic field, temperature, and so on.

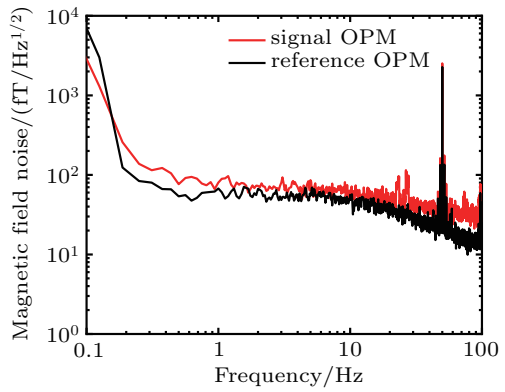

Fig. 3. Magnetic field noise of the OPMs: reference OPM (black line), signal OPM (red line).

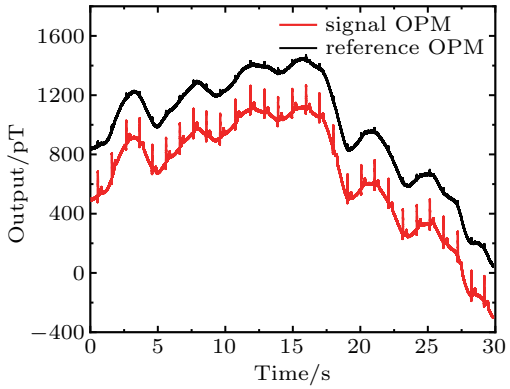

Fig. 4. Raw output of the reference (black line) and signal (red line) OPM of an adult volunteer within a moderate MSR.

Figure 4 shows the raw MCG measurements of an adult volunteer. In order to enhance the detected MCG signal, the distance between the signal OPM and the volunteer is kept to

20 mm, which is adequate for the thermal insulation and non-contact measurements. Within a moderate MSR, the fluctuation of the residual environmental fields along the z direction was about 1.5 nT. The outputs of the two OPMs aligned well with the time. The MCG signal can be sensed by the reference OPM even with a 100-mm baseline.

After the low-pass filter and synthetic gradiometer process, powerline and low-frequency interferences were effectively suppressed, as shown in Fig. 5(a). The low-frequency fluctuation was measured to be about 50 pT with a noise cancellation of 30 dB. The MCG signal can be clearly recognized. The detailed signal of about two cardiac cycle between 2.5 s to 4.5 s is shown in Fig. 5(b). The amplitude of the *R* peak was about 120 pT with an SNR of about 37 dB, which was good enough for real-time MCG measurements.

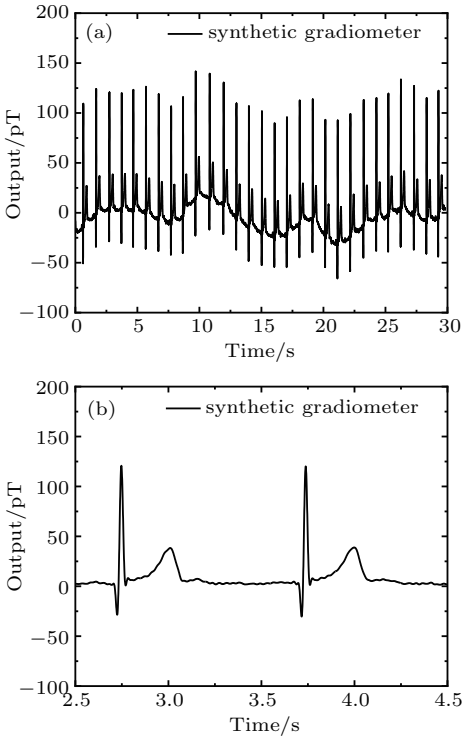

Fig. 5. (a) Real-time output of the synthetic gradiometer; (b) two cardiac MCG cycle between 2.5 s and 4.5 s.

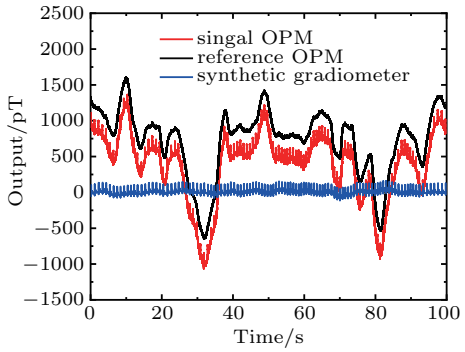

Fig. 6. Real-time recordings of the OPMs and gradiometer under a time period of 100 s: reference OPM (black line), signal OPM (red line), and synthetic gradiometer (blue line).

In order to monitor the stability of the gradiometer output, figure 6 shows a longer MCG recording of 100 s. The fluctuation of the environmental fields was measured to be about 2.2 nT. Most of the low-frequency distortion was suppressed by using the gradiometer technique. However, the residual noise was increased to be more than 100 pT. The reason may be due to the imperfect installation of the OPMs, which brings extra responses along the horizonal components of the environmental noise. Additionally, the consistency of the OPM working conditions is also an important factor. For a practical MCG system, deep studies need to be done in the near future.

4. Conclusion

In this study, we employed two OPMs to synthesize and evaluate a gradiometer technique. Under a baseline of 100 mm, noise cancelation of about 30 dB was achieved within a moderate MSR. High quality MCG signal was measured with an SNR of about 37 dB. The synthetic gradiometer technique shows to be very effective for low-frequency noise cancellation, which will be helpful to enhance the environmental field immunity. However, low-frequency distortions still exist. The next studies will be directed to improve the system stability, such as three-axial reference compensation, detailed OPM sensor characteristics, and so on.

References

[1] Geselowitz D B 1979 *IEEE Trans. Biomed. Eng.* **BME-26** 497
[2] Kwong J S, Leithäuser B, Park J W and Yu C M 2013 *Int. J. Cardiol.* **167** 1835
[3] Kwon H, Kim K, Lee Y H, Kim J M, Yu K K, Chung N and Ko Y G 2010 *Circ. J.* **74** 1424
[4] Inaba T, Nakazawa Y, Kato Y, Hattori A, Kimura T, Hoshi T, Ishizu T, Seo Y, Sato A, Sekiguchi Y, Nogami A, Watanabe S, Horigome H, Kawakami Y and Aonuma K 2017 *Supercond. Sci. Technol.* **30** 114003
[5] Park J W, Hill P M, Chung N, Hugenholtz P G and Jung F 2005 *A. N. E.* **10** 312
[6] Tao R, Zhang S L, Huang X, Tao M F, Ma J, Ma S X, Zhang C X, Zhang T X, Tang F K, Lu J P, Shen C X and Xie X M 2019 *IEEE Trans. Biomed. Eng.* **66** 1658
[7] Pizzella V, Penna S D, Gratta C D and Romani G L 2001 *Supercond. Sci. Technol.* **14** R79
[8] Kominis I K, Kornack T W, Allred J C and Romalis M V 2003 *Nature* **422** 596
[9] Shah V K and Wakai Ro T 2013 *Phys. Med. Biol.* **58** 6065
[10] Boto E, Meyer S S, Shah V, Alem O, Knappe S, Kruger P, Fromhold T M, Lim M, Glover P M, Morris P G, Bowtell R, Barnes G R and Brookes M J 2017 *NeuroImage* **149** 404
[11] Li J D, Quan W, Zhou B Q, Wang Z, Lu J X, Hu Z H, Liu G and Fang J C 2018 *IEEE Sens. J.* **18** 8198
[12] Xia H, Baranga A B A, Hoffman D and Romalis M V 2006 *Appl. Phys. Lett.* **89** 211104
[13] Boto E, Holmes N, Leggett J, Roberts G, Shah V, Meyer S S, Munoz L D, Mullinger K J, Tierney T M, Bestmann S, Barnes G R, Bowtell R and Brookes M J 2018 *Nature* **555** 657
[14] Savukov Y J, I and Newman S 2019 *Appl. Phys. Lett.* **114** 143702
[15] Li J J, Du P C, Fu J Q, Wang X T, Zhou Q and Wang R Q 2019 *Chin. Phys. B* **28** 040703